Available online at http://scik.org
Commun. Math. Biol. Neurosci. 2024, 2024:23
https://doi.org/10.28919/cmbn/8423
ISSN: 2052-2541

TOTAL NITROGEN TRANSFORMATION DYNAMICS WITH DETERMINISTIC AND STOCHASTIC YIELD COEFFICIENTS

SUNARSIH, MOCH. FANDI ANSORI*, ZANI ANJANI RAFSANJANI, SURYOTO

Department of Mathematics, Universitas Diponegoro, Semarang 50275, Indonesia

Copyright © 2024 the author(s). This is an open access article distributed under the Creative Commons Attribution License, which permits unrestricted use, distribution, and reproduction in any medium, provided the original work is properly cited.

Abstract. Nitrogen component is usually found in the wastewater and too much nitrogen will cause difficulties in managing the wastewater becoming a source of water for consumption. A natural way to reduce nitrogen in the wastewater is by planting, for example, mangroves. In this paper, we consider a dynamical system of total nitrogen transformation in a constructed wetland that has mangroves. The system has three compartments: the concentration of mangrove biomass, the concentration of total nitrogen in the wastewater, and the soil solution. In the system, there is a yield coefficient that measures how many nutrients the mangroves consume about how much biomass they produce. We study the system with deterministic linear yield and stochastic yield. For the deterministic system, we analyze the stability of the equilibria, perform some simulations to depict the phase portrait and the numerical solutions, and provide a sensitivity analysis of the yield coefficient. For the stochastic system, we present some numerical simulations of the solutions.

Keywords: constructed wetland; dynamical system; nitrogen transformation; yield coefficient.

2020 AMS Subject Classification: 37N25, 39A28.

1. INTRODUCTION

In wastewater, nitrogen compounds are frequently present, and if the wastewater is too polluted with nitrogen, the water will stink and be unsafe to drink [1]. Removing nitrogen compounds from wastewater is one area where conventional wastewater treatment systems continue

*Corresponding author

E-mail address: mochfandiansori@lecturer.undip.ac.id

Received January 02, 2024

to fall short of the current environmental standards [2]. In the meantime, wastewater treatment using constructed wetlands is seen as a replacement for conventional treatment due to its lower energy requirements, simplicity of use and maintenance, and superior therapeutic effectiveness, is spreading globally in recent years to reduce water pollution, such as nitrogen compounds removal [3, 4, 5, 6].

Constructed wetlands are a homeopathic alternative that may accurately and meticulously mimic nature and its innate characteristics and functions [7]. Constructed wetlands integrate numerous wetland ecosystem services through physical and ecological elements, such as biomass production, cooling, habitat provision, and water filtration, which entails removing nutrients like nitrogen [8, 7, 9].

The inclusion of carbon sources, such as agricultural biomass materials, can improve total nitrogen removal and significantly enhance the quality of artificial wetlands [10]. Because of their superior ability to furnish carbon and low cost, agricultural biomass materials make suitable optional carbon medium [11]. One of the plants that is widely used in constructed wetlands to provide high-quality agricultural biomass is mangroves. They can support themselves and respond differently under various environmental conditions [12, 13].

Bunwong et al. [1] proposed a model to describe the transformation of total nitrogen in a constructed wetland filled with mangroves as follows

$$\begin{cases} \dfrac{dT}{dt} = \dfrac{\beta ST}{k+S} - \sigma T \\ \dfrac{dW}{dt} = Q - (\gamma+\alpha)W \\ \dfrac{dS}{dt} = \gamma W - \dfrac{1}{Y(S)}\dfrac{\beta ST}{k+S} - \phi S \end{cases} \tag{1}$$

where T, W, and S are mangrove biomass concentration, total nitrogen concentration in the wastewater, and total nitrogen concentration in the soil solution, respectively. All the parameters β, k, σ, Q, γ, α, ϕ are positive. The explanation of these dynamics can be seen in Fig. 1. Here, $Y(S)$ is called the yield coefficient defined as a measure of how many nutrients the mangroves consume to how much biomass they produce.

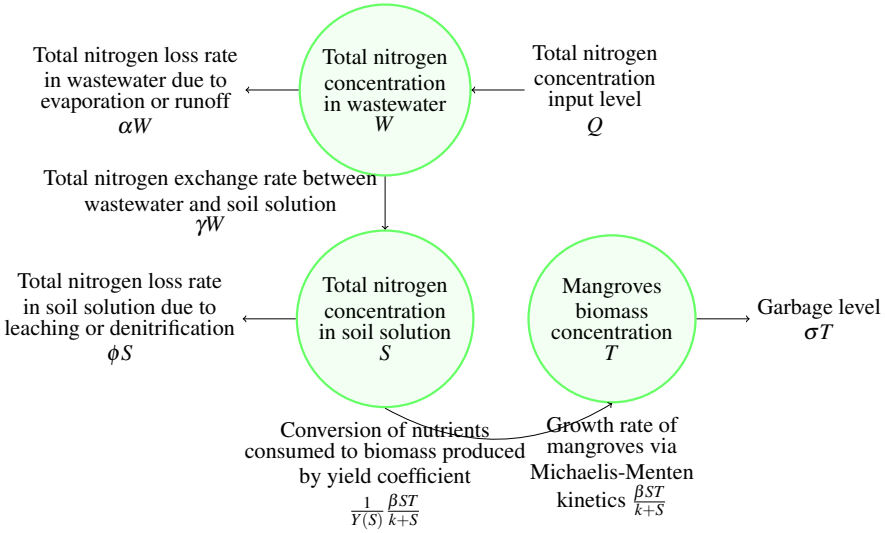

FIGURE 1. Total nitrogen transformation diagram

Bunwong et al. in [1] pointed out that the majority of earlier authors believed that the yield coefficients were traditionally constants concerning chemostats considered ecologically as a model of a simple lake [14], whereas empirical evidence has since been reported that the yield coefficient may depend on the nutrient concentration [15]. In their study, Bunwong et al. examined the model with yield coefficient $Y(S) = C + DS$, where C and D are constant, following the studies of Pilyugin and Waltman in [16] and Zhu and Huang in [15], which showed that the constant yield might be replaced by a linear function. The model of Bunwong et al. [1] has been utilized and developed by several authors for modeling other ecological engineering problems such as the study of rhizosphere microbial degradation in pollutant concentration removal [17, 18, 19, 20].

In this research, we study the Bunwong et al. model with yield coefficient $Y(S) = aS$, where $a > 0$. The equilibriums of the model and their local stability are analyzed. We also examine the sensitivity analysis for parameter a to see its impact on the model's variables. The deterministic model then is developed into the stochastic model by considering the yield coefficient is random, where the randomness appears in the parameter a, that is $Y(S) = (a + \varepsilon)S$, where ε is Gaussian white noise.

2. Model with Deterministic Yield

First, we study the model (1) with a yield coefficient defined as $Y = aS$, $a > 0$. Therefore, the model (1) becomes

$$\begin{cases} \dfrac{dT}{dt} = \dfrac{\beta ST}{k+S} - \sigma T \\ \dfrac{dW}{dt} = Q - (\gamma+\alpha)W \\ \dfrac{dS}{dt} = \gamma W - \dfrac{\beta T}{a(k+S)} - \phi S \end{cases}, \tag{2}$$

where all the parameters are described in Table 1. All the initial values are positive.

TABLE 1. Description of parameters.

Parameter	Description
β	Maximum rate of plant growth feasible given an infinite amount of total nitrogen in the soil solution
k	Semi-saturation
σ	Garbage level
Q	Total nitrogen concentration input level
γ	Total nitrogen exchange rate between wastewater and soil solution
α	Total nitrogen loss rate in wastewater due to evaporation or runoff
a	Rate of conversion of nutrients consumed to biomass produced
ϕ	Total nitrogen loss rate in soil solution due to leaching or denitrification

The equilibriums of (2) are obtained by solving $dT/dt = 0$, $dW/dt = 0$, and $dS/dt = 0$ simultaneously. We get three equilibriums as follows

$$E_1^* = \left(0, \frac{Q}{\gamma+\alpha}, \frac{\gamma Q}{\phi(\gamma+\alpha)}\right), \quad E_2^* = \left(0, \frac{Q}{\gamma+\alpha}, \frac{\sigma k}{\beta-\sigma}\right),$$
$$E_3^* = \left(\frac{ak}{\beta-\sigma}\left[\frac{\gamma Q}{\gamma+\alpha} - \frac{\phi\sigma k}{\beta-\sigma}\right], \frac{Q}{\gamma+\alpha}, \frac{\sigma k}{\beta-\sigma}\right).$$

In order to have ecological meanings, the equilibriums must be positive. Here we have positivity conditions for the equilibriums

$$\beta > \sigma \quad \text{and} \quad \frac{\gamma Q}{\gamma+\alpha} > \frac{\phi\sigma k}{\beta-\sigma}. \tag{3}$$

2.1. Local Stability Analysis. The local stability of each equilibrium is analyzed. First, we calculate the Jacobian marix of the system (2) at any point $E(T,W,S)$ as follows

$$J(E) = \begin{pmatrix} \frac{\beta S}{k+S} - \sigma & 0 & \frac{\beta k T}{(k+S)^2} \\ 0 & -(\gamma+\alpha) & 0 \\ -\frac{\beta}{a(k+S)} & \gamma & -\left(\frac{\beta T}{a(k+S)^2} + \phi\right) \end{pmatrix}. \tag{4}$$

By using the Jacobian matrix (4), we have the following theorems about the local stability of equilibriums of system (2).

Theorem 2.1. *The local stability for each of the equilibriums of system* (2) *is given as follows:*

(1) E_1^* *is stable if* $\sigma > \frac{\beta\gamma Q}{k\phi[\gamma+\alpha]+\gamma Q}$.

(2) E_2^* *is unstable.*

(3) E_3^* *is stable.*

Proof. The Jacobian matrix at equilibrium E_1^* is

$$J(E_1^*) = \begin{pmatrix} \gamma QK - \sigma & 0 & 0 \\ 0 & -(\gamma+\alpha) & 0 \\ -\frac{\phi(\gamma+\alpha)}{a}K & \gamma & -\phi \end{pmatrix},$$

where $K = \beta/(k\phi[\gamma+\alpha]+\gamma Q)$. The characteristic equation is $\lambda_1 = \gamma QK - \sigma$, $\lambda_2 = -(\gamma+\alpha)$, and $\lambda_3 = -\phi$. We have the fact that all parameters are positive, thus $\lambda_2, \lambda_3 < 0$. The equilibrium E_1^* is stable if λ_1 is also negative. This will be satisfied if $\sigma > (\beta\gamma Q)/(k\phi[\gamma+\alpha]+\gamma Q)$.

For the case of E_2^*, we have the Jacobian matrix

$$J(E_2^*) = \begin{pmatrix} 0 & 0 & 0 \\ 0 & -(\gamma+\alpha) & 0 \\ -\frac{\beta-\sigma}{ak} & \gamma & -\phi \end{pmatrix}.$$

Since this matrix is a (lower) triangular matrix, then its eigenvalues are the main diagonal. We can see that this matrix has zero eigenvalue. Thus E_2^* is not stable.

For the case of E_3^*, the Jacobian matrix is

$$J(E_3^*) = \begin{pmatrix} 0 & 0 & aL \\ 0 & -(\gamma+\alpha) & 0 \\ -\frac{\beta-\sigma}{ak} & \gamma & -\left(\frac{L}{k}+\phi\right) \end{pmatrix},$$

where $L = \frac{\beta-\sigma}{\beta}\left(\frac{\gamma Q}{\gamma+\alpha} - \frac{\phi\sigma k}{\beta-\sigma}\right)$. The characteristic equation of the Jacobian matrix is

$$0 = \lambda^3 + p_1\lambda^2 + p_2\lambda + p_3,$$

where

$$p_1 = \gamma+\alpha+\phi+\frac{L}{k}, \quad p_2 = \frac{\beta-\sigma}{k}L + (\gamma+\alpha)\left(\frac{L}{k}+\phi\right), \quad p_3 = \frac{(\gamma+\alpha)(\beta-\sigma)}{k}L.$$

The positivity conditions (3) imply $L, p_1, p_2, p_3 > 0$. From direct observation, we can see that

$$\begin{aligned} p_1p_2 &= \left[\gamma+\alpha+\phi+\frac{L}{k}\right]\left[\frac{\beta-\sigma}{k}L + (\gamma+\alpha)\left(\frac{L}{k}+\phi\right)\right] \\ &= \left[\frac{(\gamma+\alpha)(\beta-\sigma)}{k}L\right] + \left[\left(\phi+\frac{L}{k}\right)\left(\frac{\beta-\sigma}{k}L\right)\right] \\ &\quad + \left[\gamma+\alpha+\phi+\frac{L}{k}\right](\gamma+\alpha)\left(\frac{L}{k}+\phi\right) \\ &> \frac{(\gamma+\alpha)(\beta-\sigma)}{k}L = p_3. \end{aligned}$$

Thus, based on the Routh-Hurwitz stability criterion [21], i.e. the coefficients of the third-degree of polynomial characteristic equation satisfy $p_1, p_2, p_2 > 0$ and $p_1p_2 > p_3$, the equilibrium E_3^* is stable. □

2.2. Numerical Simulation of the Solution. Theorem 2.1 says that if the garbage level is too high ($\sigma > \frac{\beta\gamma Q}{k\phi[\gamma+\alpha]+\gamma Q}$), it will cause the system to converge to equilibrium E_1^*, which means the mangrove biomass concentration is zero, or in other words, it vanishes. We simulate the phase portrait and solution of system (2) in three cases when: (i) the garbage level is too high, (ii) it is not too high but not too low, and (iii) it is too low. For the third case, we will show that there exists Hopf bifurcation as shown by the appearance of the limit cycle.

For simulations, we use parameters' value: $\beta = 0.25$, $k = 1$, $Q = 1$, $\gamma = 0.15$, $\alpha = 0.2$, $\phi = 0.1$, and $a = 0.5$. These values are only for simulation purposes, but they still meet the positivity conditions in (3). We present the phase portrait of system (2) in two cases, see Fig.

2. In Fig. 2a, when the level of garbage is too high (for the simulation, we use $\sigma = 0.25$ which is greater than $\frac{\beta\gamma Q}{k\phi[\gamma+\alpha]+\gamma Q} = 0.20$), the solution-pair trajectory (T,W,S) are seen to converge to the equilibrium $E_1^* = (0, 2.86, 4.29)$ with a stable node. The clear view of the phase portrait of the system in orientation TS-plane is given in Fig. 2b.

When the level of garbage is not too high but not too low (in this case, we do simulation with $\sigma = 0.17$), in Fig. 3a, the solution-pair trajectory (T,W,S) is seen to converge to $E_3^* = (1.353, 2.857, 2.125)$ with a stable spiral. The clear view of the phase portrait of the system in orientation TS-plane is given in Fig. 3b.

When the level of garbage is too low (in this case, we simulate with $\sigma = 0.15543$), limit cycles are seen in the solution-pair trajectory (T,W,S) in Fig. 4a. Fig. 4b provides a clear view of the phase portrait of the system in the orientation TS-plane.

The solution of the system in each case is presented in Fig. 5. From the figures, we can observe the dynamics of the solution over time.

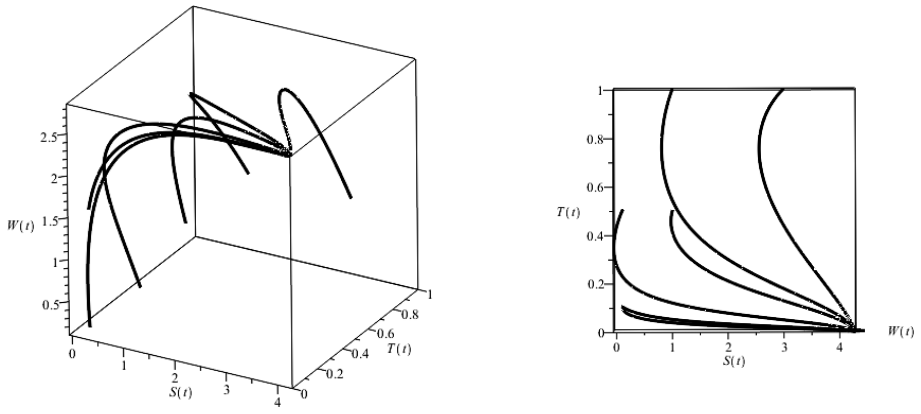

(A) (B)

FIGURE 2. (a) Phase portrait of system (2) when the level of garbage is too high, with various initial values. Panel (b) is the orientation of TS-plane showing a stable node.

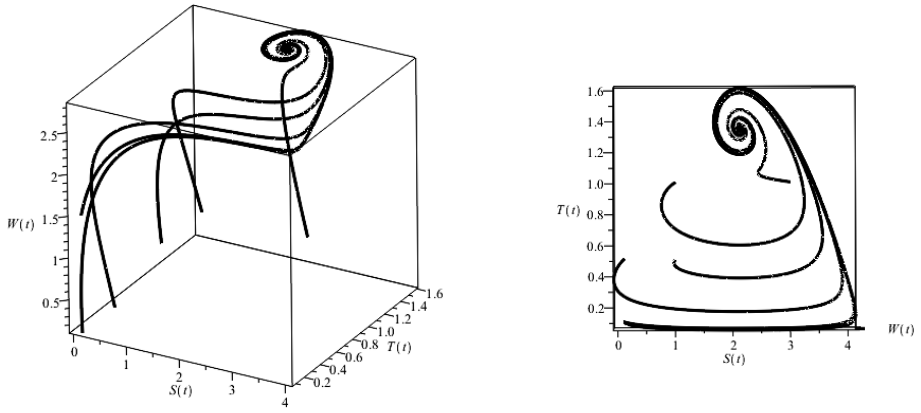

(A) (B)

FIGURE 3. (a) Phase portrait of system (2) when the level of garbage is not too high but not too low, with various initial values. Panel (b) is the orientation of TS-plane showing the stable spiral.

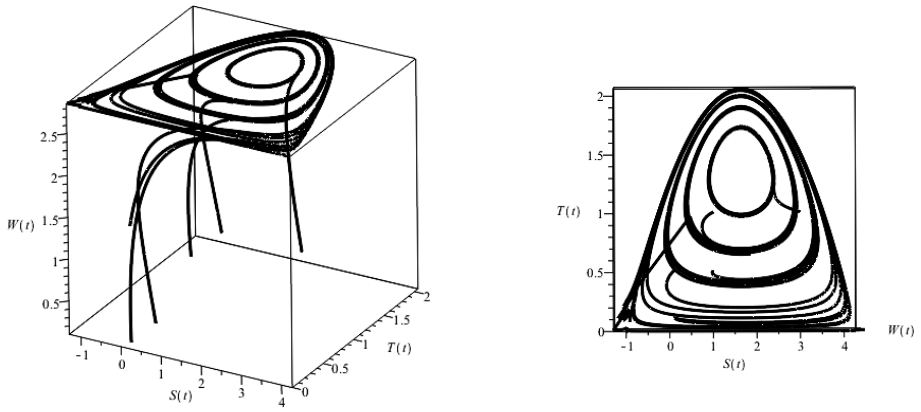

(A) (B)

FIGURE 4. (a) Phase portrait of system (2) when the level of garbage is too low, with various initial values. Panel (b) is the orientation of TS-plane showing the appearance of the limit cycle.

2.3. Sensitivity Analysis. Sensitivity analysis can give interesting qualitative behavior of a dynamical system by observing the effects of the parameters on the variables over time. This method is frequently employed in literatures [22, 23, 24, 25, 26, 27, 28, 29].

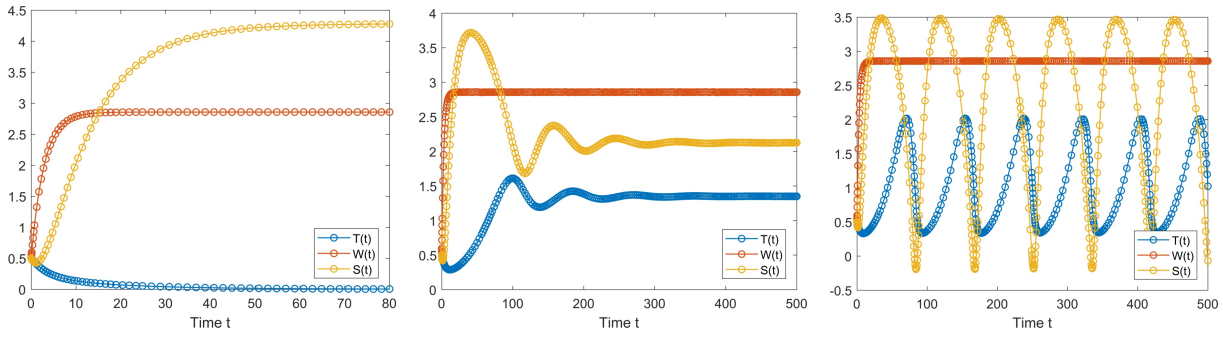

(A) (B) (C)

FIGURE 5. Numerical solution of dynamical system (2). Panel (a) is when the level of garbage is too high. Panel (b) is when the level of garbage is not too high but not too low. Panel (c) is when the level of garbage is too low.

In this paper, we focus on analyzing the sensitivity of the parameter of the yield coefficient, that is a, to the variables of the system. For the other parameters, we do not analyze them because their sensitivity has been studied in [28]. Let $X = (T,W,S)$ and define a sensitivity function $V = \frac{\partial X}{\partial a} = (\frac{\partial T}{\partial a}, \frac{\partial W}{\partial a}, \frac{\partial S}{\partial a})$. In order to simplify the writings, let $v_a^T = \frac{\partial T}{\partial a}$, $v_a^W = \frac{\partial W}{\partial a}$, and $v_a^S = \frac{\partial S}{\partial a}$. Let $\mathscr{F} = (F,G,H)$, where $F = \frac{\beta ST}{k+S} - \sigma T$, $G = Q - (\gamma+\alpha)W$, $H = \gamma W - \frac{\beta T}{a(k+S)} - \phi S$.

We have a system of ordinary differential equations of the sensitivity function as

$$\begin{aligned}
\begin{pmatrix} \frac{dv_a^T}{dt} \\ \frac{dv_a^W}{dt} \\ \frac{dv_a^S}{dt} \end{pmatrix} &= \frac{dV}{dt} = \frac{d}{dt}\frac{\partial X}{\partial a} = \frac{\partial}{\partial a}\frac{dX}{dt} = \frac{\partial \mathscr{F}}{\partial X}\frac{\partial X}{\partial a} + \frac{\partial \mathscr{F}}{\partial a} = J(X)V + \frac{\partial \mathscr{F}}{\partial a} \\
&= \begin{pmatrix} \frac{\beta S}{k+S} - \sigma & 0 & \frac{\beta kT}{(k+S)^2} \\ 0 & -(\gamma+\alpha) & 0 \\ -\frac{\beta}{a(k+S)} & \gamma & -\left(\frac{\beta T}{a(k+S)^2} + \phi\right) \end{pmatrix} \begin{pmatrix} v_a^T \\ v_a^W \\ v_a^S \end{pmatrix} + \begin{pmatrix} 0 \\ 0 \\ \frac{\beta T}{a^2(k+S)} \end{pmatrix} \\
&= \begin{pmatrix} \left[\frac{\beta S}{k+S} - \sigma\right] v_a^T + \frac{\beta kT}{(k+S)^2} v_a^S \\ -(\gamma+\alpha) v_a^W \\ -\frac{\beta}{a(k+S)} v_a^T + \gamma v_a^W - \left[\frac{\beta T}{a(k+S)^2} + \phi\right] v_a^S + \frac{\beta T}{a^2(k+S)} \end{pmatrix}
\end{aligned} \tag{5}$$

In Fig. 6, the numerical solution of the system of sensitivity function (5) is plotted versus time. In the case of too high garbage level, the parameter of yield coefficient a affects positively to both variables T and S, as shown in Fig. 6a. However, in the long run, the effect is seen disappearing. In the case of the garbage level is not too high but not too low, the yield coefficient affects positively variable S at first, but then it does not affect at all when the time goes by, as shown in Fig. 6b. In contrast, the yield coefficient stands to affect T positively as time passes. When the level of garbage is too low, the yield coefficient initially affects variable S positively, but as time passes, it has no effect. As shown in Fig. 6c, the yield coefficient is expected to have a positive effect on T as the producing limit cycle progresses.

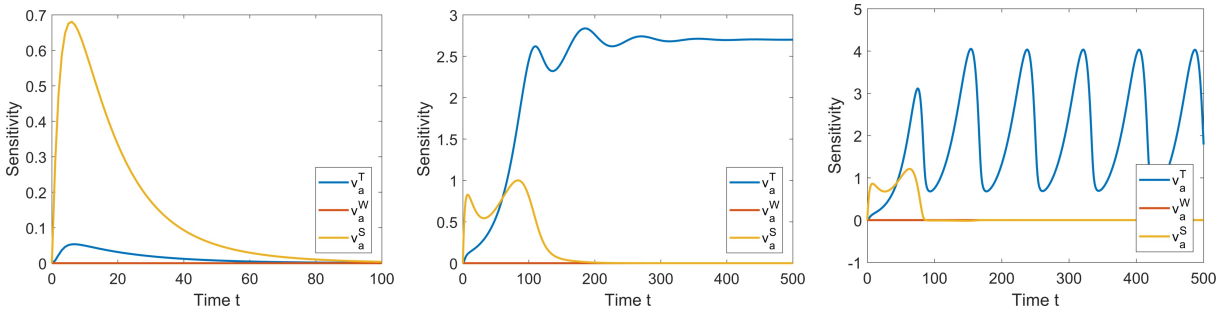

(A) (B) (C)

FIGURE 6. Sensitivity of parameter yield a to the variables. Panel (a) is when the level of garbage is too high. Panel (b) is when the level of garbage is not too high but not too low. Panel (c) is when the level of garbage is too low.

3. MODEL WITH STOCHASTIC YIELD

Now, consider the system (1) with a stochastic yield coefficient defined by $Y = (a+\varepsilon(t))S$, where $\varepsilon(t)$ is a Gaussian white noise, $\varepsilon(t) \in N(0,\sigma_\varepsilon^2)$. From Itô calculus, we have

$$(a+\varepsilon(t))dt = adt + \sigma_\varepsilon dB(t), \tag{6}$$

where $B(t)$ is a standard Wiener process.

By substituting (6) into (1) and multiplying both sides with dt, we get

$$\begin{cases} dT = \left(\dfrac{\beta ST}{k+S} - \sigma T\right) dt \\ dW = (Q - (\gamma+\alpha)W)\, dt \\ dS = (\gamma W - \phi S)\, dt - \left(\dfrac{\beta T}{k+S}\right) \dfrac{(dt)^2}{(aSdt + \sigma_\varepsilon S dB(t))} \end{cases} \tag{7}$$

To simulate the stochastic model (7), we use the Euler-Maruyama method[30] and have the following equations

$$\begin{cases} T_{t+1} = T_t + \left(\dfrac{\beta S_t T_t}{k+S_t} - \sigma T_t\right) \Delta t \\ W_{t+1} = W_t + (Q - (\gamma+\alpha)W_t)\, \Delta t \\ S_{t+1} = S_t + (\gamma W_t - \phi S_t)\, \Delta t - \left(\dfrac{\beta T_t}{k+S_t}\right) \dfrac{(\Delta t)^2}{(a\Delta t + \sigma_\varepsilon B_t(\Delta t))} \end{cases} \tag{8}$$

where $B_t(\Delta t) \in N(0, \Delta t)$.

Similarly with previous simulations in Fig. 6, we simulate the stochastic model in three cases based on the level of garbage. The stochastic model's simulation uses $\Delta t = 1$. In Fig. 7a, by using standard deviation $\sigma_\varepsilon = 0.4$, we simulate the stochastic model in the case of garbage level is too high. Meanwhile in Figs. 7b and 7c, by using standard deviation $\sigma_\varepsilon = 0.05$, we simulate the stochastic model in the case of garbage level is not too high but not too low and when it is too low, respectively. From the figures, we can observe that the randomness in yield coefficient mostly affects the variable S, the total nitrogen concentration in soil solution, rather than the variable T.

4. CONCLUSION

The stability of the system of total nitrogen transformation in a constructed wetland can be observed through the level of garbage. When the level of garbage is too high, the mangrove biomass will vanish. When the level of garbage is not too high, the system may be a stable spiral or stable limit cycle.

The yield coefficient affects positively to the mangrove biomass concentration dynamics over time with the sensitivity depending on the system's behavior when reaching the equilibrium

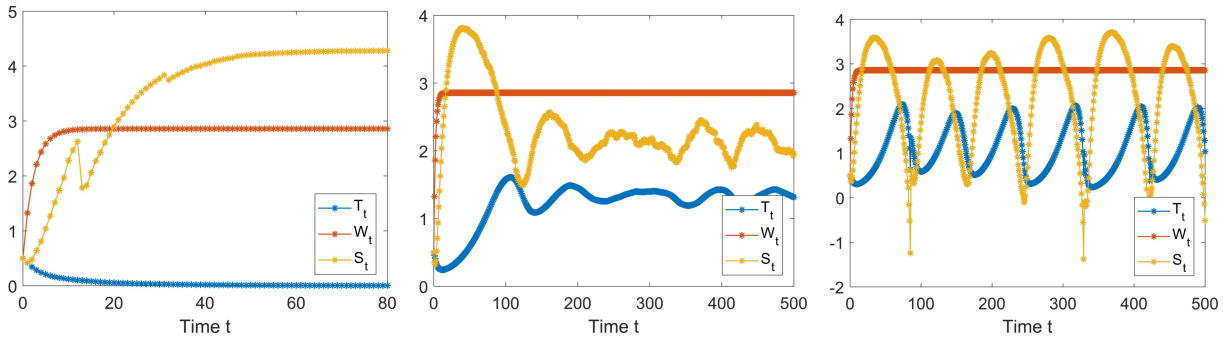

(A) (B) (C)

FIGURE 7. Numerical solution of stochastic model (7). Panel (a) is when the level of garbage is too high. Panel (b) is when the level of garbage is not too high but not too low. Panel (c) is when the level of garbage is too low.

(stable spiral or stable limit cycle). The yield coefficient also affects positively the total nitrogen concentration in soil solution over time but in a long time, it does not affect at all.

When the system is studied with a stochastic yield coefficient, the numerical simulations show that the dynamics of total nitrogen concentration in soil solution change drastically compared with the dynamics of mangrove biomass concentration.

ACKNOWLEDGMENTS

The authors would like to thank Direktorat Riset, Teknologi dan Pengabdian Masyarakat (DRTPM) Dirjenristek Kemendikbudristek Indonesia for sponsoring the study with grant number SPK: 449-23/UN7.D2/PP/VI/2023.

CONFLICT OF INTERESTS

The authors declare that there is no conflict of interests.

REFERENCES

[1] K. Bunwong, W. Sae-jie, Y. Lenbury, Modelling nitrogen dynamics of a constructed wetland: Nutrient removal process with variable yield, Nonlinear Anal.: Theory Methods Appl. 71 (2009), e1538–e1546. https://doi.org/10.1016/j.na.2009.01.230.

[2] H. Wu, J. Zhang, H.H. Ngo, et al. A review on the sustainability of constructed wetlands for wastewater treatment: Design and operation, Bioresource Technol. 175 (2015), 594–601. https://doi.org/10.1016/j.biortech.2014.10.068.

[3] M.A. Senzia, D.A. Mashauri, A.W. Mayo, Suitability of constructed wetlands and waste stabilisation ponds in wastewater treatment: nitrogen transformation and removal, Phys. Chem. Earth, Parts A/B/C. 28 (2003), 1117–1124. https://doi.org/10.1016/j.pce.2003.08.033.

[4] N.S. Strigul, L.V. Kravchenko, Mathematical modeling of PGPR inoculation into the rhizosphere, Environ. Model. Softw. 21 (2006), 1158–1171. https://doi.org/10.1016/j.envsoft.2005.06.003.

[5] L. Jia, E. Gou, H. Liu, et al. Exploring utilization of recycled agricultural biomass in constructed wetlands: characterization of the driving force for high-rate nitrogen removal, Environ. Sci. Technol. 53 (2019), 1258–1268. https://doi.org/10.1021/acs.est.8b04871.

[6] Z. Han, J. Dong, Z. Shen, et al. Nitrogen removal of anaerobically digested swine wastewater by pilot-scale tidal flow constructed wetland based on in-situ biological regeneration of zeolite, Chemosphere. 217 (2019), 364–373. https://doi.org/10.1016/j.chemosphere.2018.11.036.

[7] H. Choi, F.K. Geronimo, M. Jeon, et al. Evaluation of bacterial community in constructed wetlands treating different sources of wastewater, Ecol. Eng. 182 (2022), 106703. https://doi.org/10.1016/j.ecoleng.2022.106703.

[8] H. Choi, F.K.F. Geronimo, M. Jeon, et al. Investigation of the factors affecting the treatment performance of a stormwater horizontal subsurface flow constructed wetland treating road and parking lot runoff, Water. 13 (2021), 1242. https://doi.org/10.3390/w13091242.

[9] D.P.L. Rousseau, F. Louage, Q. Wang, et al. Constructed wetlands for urban wastewater treatment: an overview, in: Encyclopedia of Inland Waters, Elsevier, 2022: pp. 272–284. https://doi.org/10.1016/B978-0-12-819166-8.00108-0.

[10] Y. Zhang, M. Li, L. Dong, et al. Effects of biochar dosage on treatment performance, enzyme activity and microbial community in aerated constructed wetlands for treating low C/N domestic sewage, Environ. Technol. Innov. 24 (2021), 101919. https://doi.org/10.1016/j.eti.2021.101919.

[11] L. Jia, C. Li, Y. Zhang, et al. Microbial community responses to agricultural biomass addition in aerated constructed wetlands treating low carbon wastewater, J. Environ. Manage. 270 (2020), 110912. https://doi.org/10.1016/j.jenvman.2020.110912.

[12] Y. Wu, A. Chung, N.F.Y. Tam, et al. Constructed mangrove wetland as secondary treatment system for municipal wastewater, Ecol. Eng. 34 (2008), 137–146. https://doi.org/10.1016/j.ecoleng.2008.07.010.

[13] J.Y.S. Leung, Q. Cai, N.F.Y. Tam, Comparing subsurface flow constructed wetlands with mangrove plants and freshwater wetland plants for removing nutrients and toxic pollutants, Ecol. Eng. 95 (2016), 129–137. https://doi.org/10.1016/j.ecoleng.2016.06.016.

[14] X. Huang, L. Zhu, A three dimensional chemostat with quadratic yields, J. Math. Chem. 38 (2005), 575–588. https://doi.org/10.1007/s10910-005-6908-0.

[15] L. Zhu, X. Huang, Multiple limit cycles in a continuous culture vessel with variable yield, Nonlinear Anal.: Theory Methods Appl. 64 (2006), 887–894. https://doi.org/10.1016/j.na.2005.05.049.

[16] S.S. Pilyugin, P. Waltman, Multiple limit cycles in the chemostat with variable yield, Math. Biosci. 182 (2003), 151–166. https://doi.org/10.1016/s0025-5564(02)00214-6.

[17] Z. Zhao, L. Pang, Z. Zhao, et al. Impulsive state feedback control of the rhizosphere microbial degradation in the wetland plant, Discr. Dyn. Nat. Soc. 2015 (2015), 612354. https://doi.org/10.1155/2015/612354.

[18] Z. Zhao, Y. Song, L. Pang, Mathematical modeling of rhizosphere microbial degradation with impulsive diffusion on nutrient, Adv. Differ. Equ. 2016 (2016), 24. https://doi.org/10.1186/s13662-015-0720-3.

[19] Z. Zhao, Q. Li, L. Chen, Effect of rhizosphere dispersal and impulsive input on the growth of wetland plant, Math. Computers Simul. 152 (2018), 69–80. https://doi.org/10.1016/j.matcom.2018.04.003.

[20] Z. Zhao, Y. Chen, Q. Li, et al. Mathematical model for diffusion of the rhizosphere microbial degradation with impulsive feedback control, J. Biol. Dyn. 14 (2020), 566–577. https://doi.org/10.1080/17513758.2020.1786860.

[21] S. Salivahanan, R. Rengaraj, G.R. Venkatakrishnan, Control systems engineering, Pearson India Education Services, Chennai, Delhi, 2015.

[22] D. Suandi, I.P. Ningrum, A.N. Alifah, et al. Mathematical modeling and sensitivity analysis of the existence of male calico cats population based on cross breeding of all coat colour types, Commun. Biomath. Sci. 2 (2019), 96. https://doi.org/10.5614/cbms.2019.2.2.3.

[23] D. Suandi, K.P. Wijaya, M. Amadi, et al. An evolutionary model propounding Anopheles double resistance against insecticides, Appl. Math. Model. 106 (2022), 463–481. https://doi.org/10.1016/j.apm.2022.01.025.

[24] K.Z. Mapfumo, J.C. Pagan'a, V.O. Juma, et al. A model for the proliferation-quiescence transition in human cells, Mathematics. 10 (2022), 2426. https://doi.org/10.3390/math10142426.

[25] F. Rentzeperis, D. Wallace, Local and global sensitivity analysis of spheroid and xenograft models of the acid-mediated development of tumor malignancy, Appl. Math. Model. 109 (2022), 629–650. https://doi.org/10.1016/j.apm.2022.05.006.

[26] S. Alsahafi, S. Woodcock, Exploring HIV dynamics and an optimal control strategy, Mathematics. 10 (2022), 749. https://doi.org/10.3390/math10050749.

[27] V. Reinharz, A. Churkin, H. Dahari, et al. Advances in parameter estimation and learning from data for mathematical models of hepatitis C viral kinetics, Mathematics. 10 (2022), 2136. https://doi.org/10.3390/math10122136.

[28] Sunarsih, M. Ansori, S. Khabibah, et al. Continuous and discrete dynamical models of total nitrogen transformation in a constructed wetland: sensitivity and bifurcation analysis, Symmetry. 14 (2022), 1924. https://doi.org/10.3390/sym14091924.

[29] J. Nainggolan, M.F. Ansori, Stability and sensitivity analysis of the COVID-19 spread with comorbid diseases, Symmetry. 14 (2022), 2269. https://doi.org/10.3390/sym14112269.

[30] D.J. Higham., An algorithmic introduction to numerical simulation of stochastic differential equations, SIAM Rev. 43 (2001), 525–546. https://doi.org/10.1137/s0036144500378302.